Received: July 24, 2024. Revised: August 17, 2024. 1016

International Journal of
Intelligent Engineering & Systems

http://www.inass.org/

Gain Improvement of Millimetre-Wave Two Element Array Antenna for 5G Networks by Using Frequency-Selective Surface-based Reflector

Nada Nasih Tawfeeq[1]* **Adheed Hasan Sallomi[1]**

[1] *Electrical Department, Mustansiriyah University, Baghdad, Iraq*
* Corresponding author's Email: nada.nasih@uomustansiriyah.edu.iq

Abstract: This article proposes a two-element antenna array integrated with a reflector based on Frequency Selective Surface (FSS) of single layer to achieve a significant gain. Each of the antenna elements receives power from an individual port. The FSS-based reflector comprises 7 × 7 unit cells, each of which measures 2.8 x 2.8 mm^2 and exhibits multiband behaviour. The antenna is built on a Rogers RT-5880 substrate with a broad frequency range that spans 25 GHz to 30.3 GHz and 57.5 GHz to 80 GHz, encompassing millimetre wave bands (n275, V, and E) band. The suggested reflector exhibits stop-band transmission characteristics under the limit of -10 dB between 21.1 GHz - 31.3 GHz and 47.65 GHz - 80 GHz. The two-element antenna is combined with the proposed reflector, increasing gain from 6.7 to 11.1 dBi at 28 GHz, 8.7 to 10.75 dBi at 60 GHz, and 8.5 to 9.49 dBi at 73 GHz. The antenna's measurements are 20 x 16.5 x 0.87 mm^3. The suggested antenna exhibits steady gain and directed radiation patterns. The modelling outcomes are validated realistically by examining the built prototypes of the suggested antenna design.

Keywords: FSS-based reflector, Millimeter-wave antenna, Gain improvement.

1. Introduction

The advancements of wireless data transmission technology currently have created a major change in the wireless industry [1]. The growing need for more capacity, rapid data rates, robust connection, and support for an enormous customer base is driving this expansion [2]. 5G technological advancements have been essential in meeting these objectives by offering the required bandwidth and information speeds [3]. Studies and research indicate that a couple of common frequency ranges have been designated for the technology known as 5G. These consist of the top band, also referred to as millimeter waves, and the second band, which is less than 6 GHz. Since there are now numerous uses utilizing the sub-6 GHz band, real communication for millimeter waves using unlicensed and unconstrained bandwidth must be established [4-5]. Frequencies like 28 and 38 GHz within the millimeter-wave spectrum are considered as possible options for next fifth generation standards in comparison to other millimeter frequency range, due to the improved propagation and less complicated devices. [6-7]. Researchers started developing transceivers for 5G cellular communication systems [8-9]. To facilitate fast wireless communications over short distances, the unlicensed spectral range between 59 and 64 GHz was assigned by the Federal Communication Commission (FCC) [10]. The frequency spectrum at 60 GHz is particularly significant due to the wide bandwidth of 7-9 GHz available in the unlicensed spectrum. Recognizing the importance of efficient utilization of the 70/80/90 GHz bands, the FCC has supported amendments that allow the use of compact antennas to serve as the wireless backbone for 5G networks [11]. Improved bandwidth and data speeds and bandwidth may be accomplished by utilizing a larger percentage of the spectral range, but this comes with the risk of environmental attenuation from elements like rain, fog, and snow. High-gain and directed antennas can be utilized to get better performance in the millimeter-wave bands by overcoming these atmospheric attenuation-related difficulties.

There are several techniques were employed to improve the antenna directivity and gain; these techniques including a conductor with artificial magnetic characteristics (AMC) beneath the radiator [12-15], A rectangular monopole antenna with gain of 4.86 dBi was proposed in [12] using AMC surface with a ring monople antenna at 28 GHz, the gain enhanced up to 8.59 dBi. In [13], a slotted-bowtie shaped antenna with artificial magnetic conductor unit cells was developed to achieve a gain of 5.5dBi. In [14], a yagi antenna operating at 60 GHz gain improved by only 2.5 dB with the introduction of Jerusalem Cross-AMC. Furthermore, an AMC-ground based antenna covering the 28 GHz and 38 GHz with gain of 6.92 dBi [15]. According the above studies, the gain improvement capability of (AMCs) in millimeter-wave bands is more substantial for antennas operating at a single frequency, rather than antennas with multiple frequency bands. The antenna gain also can be improved by using a high number of antenna elements [16-19]. For instance, an array of 16 element circular patch antenna that operates at 28 GHz showed a gain value of 16.58 dBi described in [16]. Another 16 elements antenna resonates at 60 GHz also shows high gain of 16.5 dBi in [17]. In [18], a planar antenna array of 8 elements is presented with multiple slots and I-shape cuts on the ground plane operate in the two bands of 26 GHz and 28 GHz. The antenna gain reached 13.22 dBi due to the array arrangement and additional modifications. Furthermore, the work in [19] demonstrated an antenna array of 2 elements operated at two bands of 28 GHz and 38GHz with gain of 10.5 dBi at each. As indicated earlier, while antenna arrays can help improve overall gain, there are trade-offs involved either the array takes up a large physical space, or the bandwidth over which the gain improvement is realized is relatively narrow. Another method to improve the antenna gain is the utilization of FSS for millimeter-wave applications. For this, an Ultra Wide Band (UWB) antenna is proposed in [20] with L shaped FSS unit cell. A peak gain of 8.24 dBi is achieved. Furthermore, in [21], a Fabry–Perot cavity antenna based on a metasurface known as bianisotropic is designed that work at 28 GHz. The outcome reports a peak gain of 14.1 dBi. In [22], two techniques based on an array of 8 elements of wide bandwidth mounted and a FSS layer were combined to operate at the millimeter wave band and accomplish a gain of 15dBi.

In this work, two techniques are employed to enhance the antenna gain. The addition of a second antenna array element increases the gain by approximately 3 dB. Furthermore, the integration of an FSS-based reflector provides an additional 3 dB improvement in gain. Compared to the other designs presented, this work has maintained a compact size while still achieving an improved gain performance and a wider operating bandwidth. The initial antenna configuration is based on a previous work in [23]. The resultant single element exhibits multiband characteristics spanning frequencies of (25.41-31.96) GHz and (35.16-80) GHz. Although the single-element antenna exhibits good radiation patterns, it is limited to low gain values (i.e., 4 dBi, 5 dBi, and 6.2 dBi) at n257, V, and E bands. The antenna with single element is converted into a two-element antenna to accommodate the elevated gain demand while remaining small. The two elements of the optimum layout indicate peak gain levels of 6.7 dBi, 8.7 dBi, and 8.5 dBi. Unit cell metamaterial has been developed to enhance the gain even further. A single-layer reflector based on frequency selective surface comprised of 7x7 unit cells is created to obtain even more gain enhancement. The two-element antenna's rear side is equipped with an FSS-based reflector, spaced 2 mm apart. Gain values of 11.1 dBi at 28 GHz, 10.75 dBi at 60 GHz, and 9.49 dBi at 73 GHz show an adequate increase. The suggested arrays of antenna and reflector layouts were constructed. Both the modelled and verified outcomes accord well. The following parts of the article are structured as outlined next: The second section examines the structure and development of the two-element antenna. The third section focused on the unit cell structure and associated FSS-based reflector array. The fourth section demonstrated an analysis of simulated and fabricated designs. The fifth section includes an analysis of the proposed design to relevant work. The final section offers the conclusion of the suggested work.

2. Design and development of the two element antenna

The following paragraph provides an in-depth description of the stages required in designing a two-element antenna. The single-element is developed into two-element designs to fulfil the demands of applications for 5G. A substrate termed Rogers RT-5880 with a 0.8 mm height, a 2.2 relative permittivity, and a 0.0009 loss tangent has been employed.

According to [23], the antenna design has taken four design modes, the third mode known as Mode-C is investigated in this study due to the fact is covers the targeted bands, thereby further analysis has taken place. The single-element design has suitable radiation pattern properties, but its small gain values are a constraint. Thus, as displayed in Fig. 1, a single-element configuration is developed to two-element to

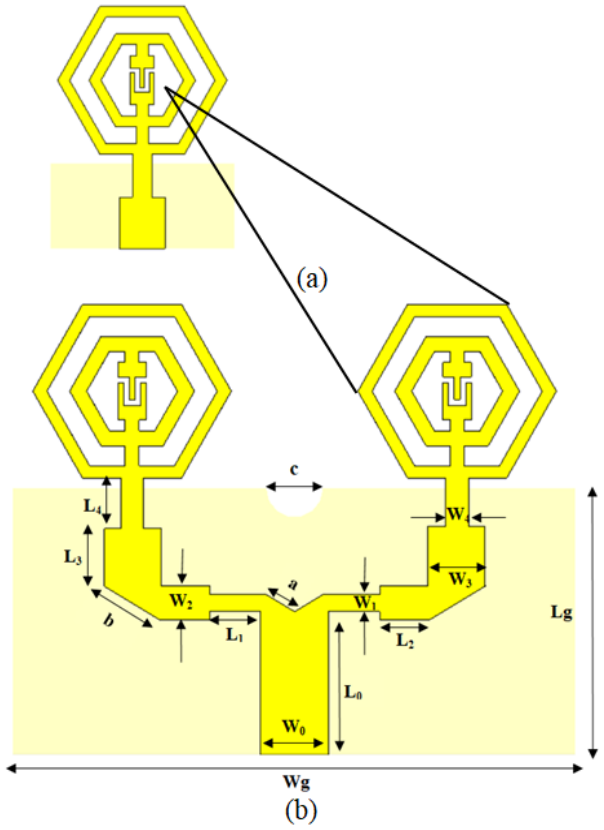

Figure. 1 Layout of the suggested antenna: (a) single-element reported in [23] and (b) developed two-element antenna geometries

compensate the requirement for a greater gain needed for 5G applications.

The specified distance between the individual element's inter-elements is 9.4 mm to obtain a wide-angle radiation pattern. Since lower frequencies require greater inter-element distances to mitigate mutual coupling compared to higher frequencies, the lower frequency was selected as frequency of reference to calculate the inter-element distance without coupling between them [22]. For the 1x2 array feeding point, a T-type junction was selected due to its simplicity in manufacturing and design. This junction serves to split the injected signal's power equally, with impedances of 100, 50, and 100 Ω. Quarter-wave transformers with an impedance of 70 Ω are implemented on both ends of the junction. The following equations from Eq. (1) to Eq. (2) have been used to determine the feeding line widths and lengths [24]:

$$\frac{W_n}{h} = \begin{cases} \dfrac{8e^A}{e^{2A}-2}, & \dfrac{W_n}{h} < 2 \\ \dfrac{2}{\pi}\left[B-1-\ln(2B-1) + \dfrac{\varepsilon_r-1}{2\varepsilon_r}\left\{\ln(B-1)+0.39-\dfrac{0.61}{\varepsilon_r}\right\}\right], & \dfrac{W_n}{h} > 2 \end{cases} \quad (1)$$

$$A = \frac{Z_0}{60}\sqrt{\frac{\varepsilon_r+1}{2}} + \frac{\varepsilon_r-1}{\varepsilon_r+1}\left(0.23+\frac{0.11}{\varepsilon_r}\right) \quad (2)$$

Where ε_r is the substrate dielectric constant

$$B = \frac{377\pi}{2Z_0\sqrt{\varepsilon_r}} \quad (3)$$

$$L_n = \frac{\phi f_c(\frac{\pi}{180})}{\sqrt{\varepsilon_{reffLn}}k_0} \quad (4)$$

$$\varepsilon_{reffn} = \frac{\varepsilon_r+1}{2} + \frac{\varepsilon_r-1}{2}\frac{1}{\sqrt{1+12\frac{h}{W_n}}} \quad (5)$$

L_n, W_n present the length and width of the feeding lines in three cases: First, Z_0=50 Ω when (n=0, 3). Second, Z_0=100 Ω (n=1). Finally, Z_0=70 Ω (n=2, 4). The width of the T-junction is determined by each line-impedance and the "V" geometry with value "a"

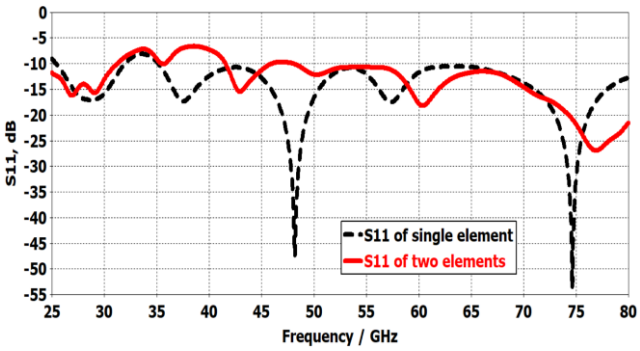

Figure. 2 Compared S-parameter (S11) of suggested (single/two) element antenna design

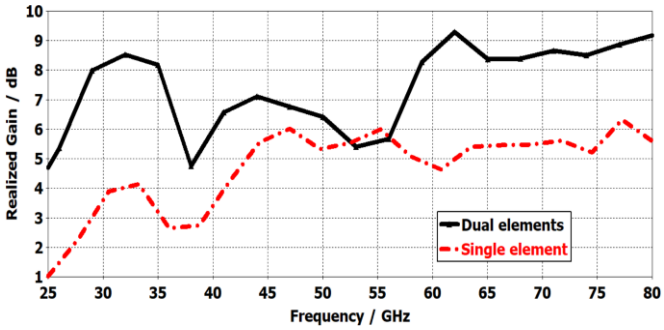

Figure. 3 Compared realized gain of the suggested (single/two) element antenna designs

Table 1. Measurements of the suggested antenna

Parameters	W_0	L_0	W_1	L_1	a
Value (mm)	2.4	5	0.6	1.8	1.17
Parameters	W_2	L_2	W_3	L_3	b
Value (mm)	1.2	1.73	2	2	2.33
Parameters	W_4	L_4	Wg	Lg	c
Value (mm)	0.8	1.77	20	9.3	2

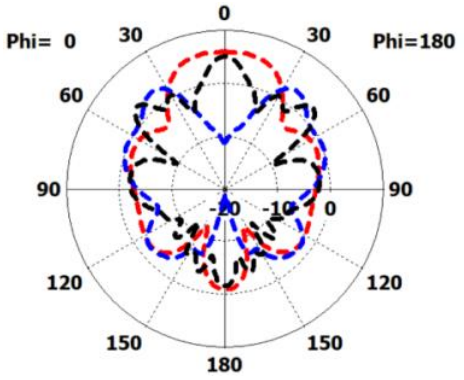

(a)

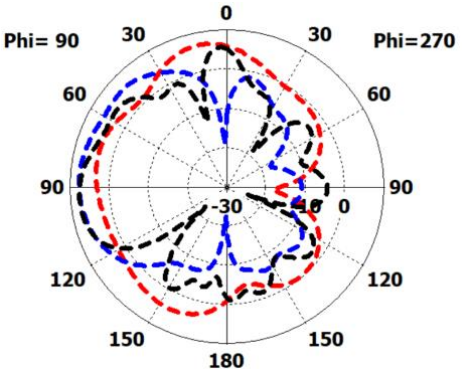

(b)

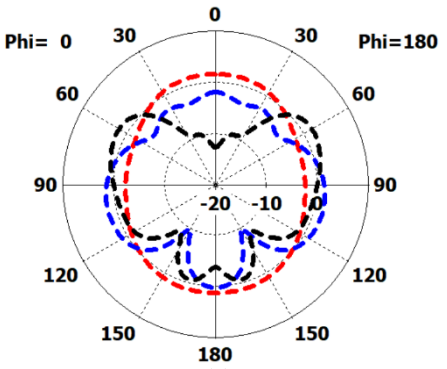

(c)

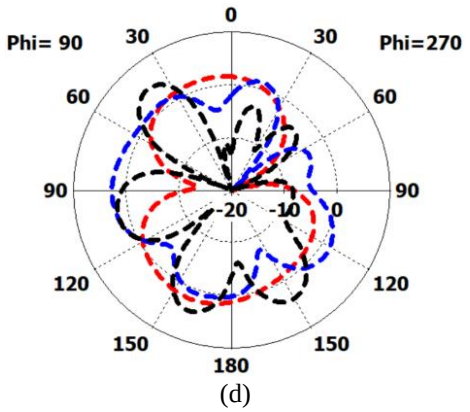

(d)

Figure. 4 Radiation patterns comparison: (a) Single element E-Plane (b) Single element H-Plane (c) Two elements E-Plane, and (d) Two elements H-Plane where Red (28 GHz), Blue (60 GHz) and Black (73 GHz)

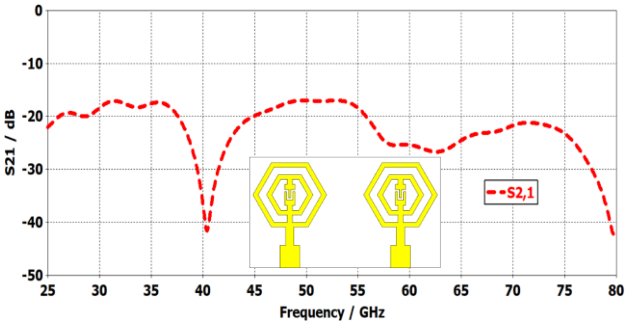

Figure. 5 S-parameter (S21) of two-element antenna

is required to reduce the parasitic reactance which results from the junction's discontinuity. According to [25], "a" value should be 1.8 of the feeder width. Table 1 displays the feed lines network details for the suggested antenna.

Figs. 2, 3, and 4 illustrate the simulation of S11, gain with frequency, and radiation patterns for the two-element antennas. Fig. 2 shows some variance in impedance (S11 < -10 dB) between single and two-element configurations where the second band is shifted to (41.37-80) GHz with a stop band of 1.4 GHz from (46.22-47.62) GHz. Such variation is acceptable due to the fact it covers the essential bands taken in this study. As the number of elements changes to two, the gain value also increases through the band. Fig. 3 displays an analysis of radiation patterns in both (E and H) planes, demonstrating that gain increases in tandem with the array elements number.

To measure the mutual coupling within nearby elements, the two elements are supplied by individual power supply rather than one feeding line, as shown in Fig. 5. It is essential to note that there is low mutual coupling between components due to sufficient separation between neighbouring elements.

3. Design of reflector unit cell configuration

Frequency Selective Surface is one- or two-dimensional periodic patterns that replicate. Unit cells in FSS are arranged in a repetitive pattern. Based on their construction, FSS structures can transmit, absorb, or reflect electromagnetic radiation [26]. Because of its wideband responsiveness, high angular and polarization stability, and structural simplicity, a number of circular ring structures are combined in this research study to create the suggested FSS. Multi rings for multi-band operations may be effectively arranged in this configuration while maintaining a tiny footprint, which enables the construction of numerous unit cells in a condensed area. A 2.8 x 2.8 mm^2 unit cell was designed using a FR-4 substrate with 1.6 mm height. Unit cell modeling in CST has been performed to acquire a broad bandwidth that

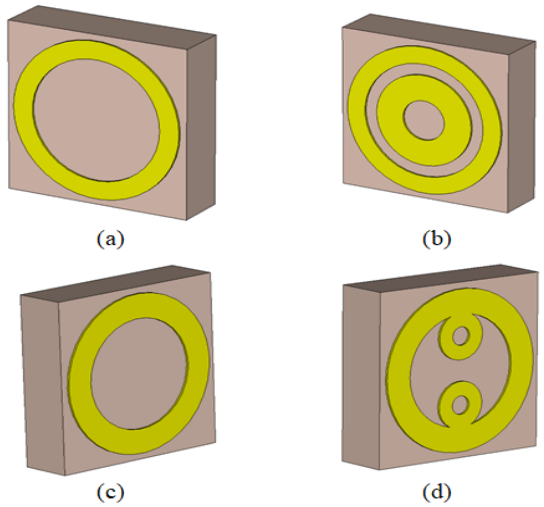

Figure. 6 Optimization of the unit cell (a) front side single ring, (b) front side optimized unit cell, (c) back side single ring, and (d) back side optimized unit cell

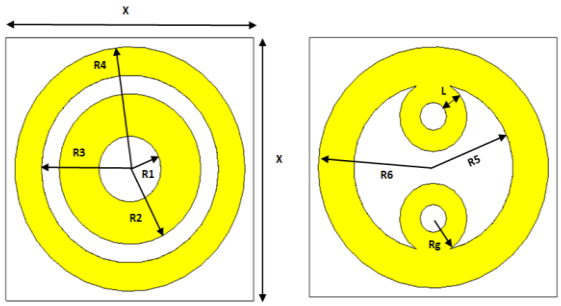

Figure. 7 Optimized structure FSS: (a) front view with cell configuration (X=2.8, R1=0.35mm, R2=0.8mm, R3=1 mm, R4=1.3mm) and (b) back view (R5=0.9mm, R6=1.3mm, Rg=0.38mm, L=0.23mm)

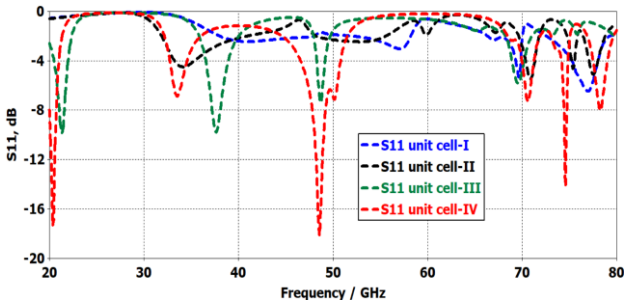

Figure. 8 Comparison of S-parameter (S11) of the different unit cell design steps

encompasses all of the desired bands. The progression of unit cell design for the targeted frequencies results in the final front and back structure of the unit cell shown in Fig. 6. (b) and (d). The unit cell-I with single ring shape only enables operation in two bands. It may exhibit stop-band behavior at 60 GHz from 58.5 GHz to 60.8 GHz and band stop behavior at 28 GHz with 14 GHz bandwidth from 20 GHz to 34 GHz, with the constraint of covering 73 GHz. Two stop band characteristics are also displayed by unit cell-II with the introduction second ring. These encompass 28 GHz and 73 GHz bot the 60 GHz is not covered at S21 < -10 dB. Unit cell-III's design is designed to cover all targeted bands, including 60 GHz, but it also exhibits restricted operating behavior, covering just 28 GHz with a 13.3 GHz bandwidth from (22.7 – 36) GHz. The optimum unit cell-IV design is intended to display stop band behavior with better S21 < -10 throughout all targeted bands from (21.1-31.3) GHz, (54.2-63.6) GHz, and (65-75) GHz. Fig. 7 demonstrates the final structure of the FSS based reflector at the intended frequencies. Figs. 8 and 9 provide a comparison of S11 and S21 for all unit cells.

The advanced design system (ADS) software is employed to verify the equivalent circuit, and the outcomes of the CST simulation are contrasted as can be seen in Fig. 10. Each ring based on three series inductor, capacitor, and resistor [27]. The first two RLC diagrams represent the rings located on the top of the FSS reflector, a mutual coupling, represented as inductance between the rings [28].

The ground plane is also presented by a series RLC. The dielectric substrate acts as an impedance converter to facilitate the impedance conversion of parallel inductor and capacitor [29]. To verify the precision of the equivalent circuit model, Fig. 11 illustrates a comparison between the S-parameters obtained from CST MWS and ADS software packages. The comparison demonstrates an excellent agreement between the two software outcomes. Table 2 presents the equivalent circuit components values. To obtain high gain, the 7x7 unit cells FSS-based reflector array of is implemented with an optimal spacing of 2 mm from the rear end of the two-element antenna design, as displayed in Fig. 12. The space value chosen to be higher than λ/4 where (λ is the wavelength of the signal) to achieve in phase reflection at 28 GHz. The antenna's combined dimension with FSS-based reflector has altered a little, to 19.6 x20 x 5.54 mm^3. Due to its compact size, the suggested integrated antenna is suitable for use in any smartphone. The gains were improved by 4 dB, 2 dB, and 1.2 dB at n257, V, and E-bands, respectively. Fig. 13 displays a comparison of gain with and without FSS. Gains are clearly increased at the targeted bands while the antenna's general characteristics remain unchanged. Specific parametric research was conducted to determine the optimal spacing of 2 mm between the antenna and reflector. The suggested two-element antenna employing FSS has the highest gain compared to other antenna layouts and is regarded a viable antenna for 5G communications. The proposed configuration is built, and the simulation outcomes are carefully

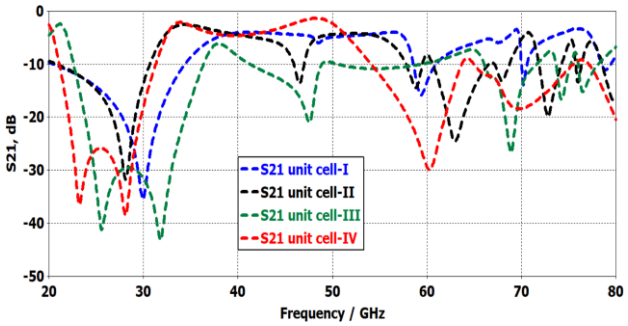

Figure. 9 Comparison of S-parameter (S21) of the different unit cell design steps

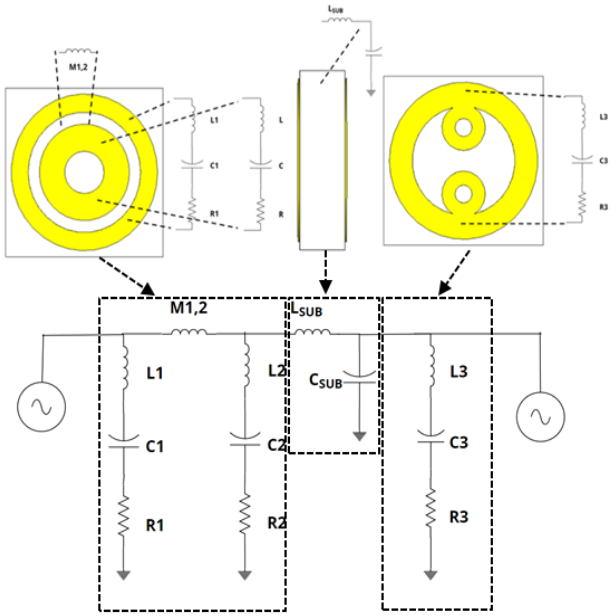

Figure. 10 The unit cell equivalent circuit configuration: (a) unit cell model in CST and (b) equivalent circuit in ADS

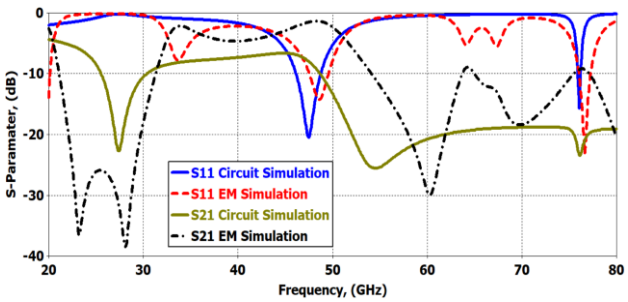

Figure. 11 Simulated S-parameters outcomes of the suggested reflector single cell

compared and confirmed at the measuring facility.

The impact of the introduction of the reflector is examined and the overall radiation efficiency is presented for the three targeted bands of interest with and without the FSS in Fig. 14. Without the suggested FSS layout, the antenna exhibits efficiencies of approximately 92%, 88%, and 90% at the bands of interest, sequentially. While, the antenna radiation efficiencies based on the proposed FSS reflector are reduced to 90%, 85%, and 86% at the same bands. The antenna efficiency is reduced due to the introduction of additional conductors and dielectric material losses.

4. Outcomes of the fabricated antenna integrated with FSS-based reflector

Fig. 15 represents the fabrication of a two-element array with an FSS reflector. The estimated findings, involving return loss and radiation pattern, are checked in the measuring lab. Fig. 16 shows a comparison of estimated and observed S-parameter (S11) which is in close agreement. The tested and estimated radiation pattern outcomes of the antenna at 28, 60, and 73 GHz in the (E and H) planes are displayed in Fig. 17. Some improvements are noticed in the radiation patterns, with more directed, symmetrical, and concentrated forms compared to the radiation pattern without reflector in Fig. 4. This demonstrates how well the design refining process worked to create an ideal dual-band millimeter-wave reflector and antenna system. The strong similarity between the estimated and tested findings validates the design strategy and gives assurance about the performance of the antenna system in next-generation wireless applications.

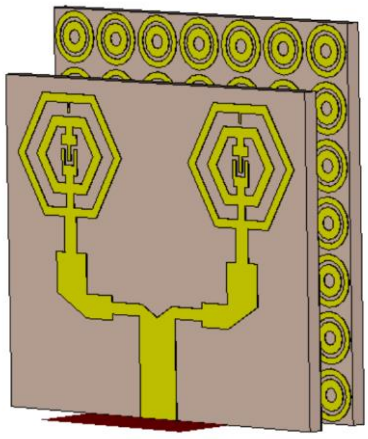

Figure. 12 Perspective graphic of the planned antenna mounted with the FSS

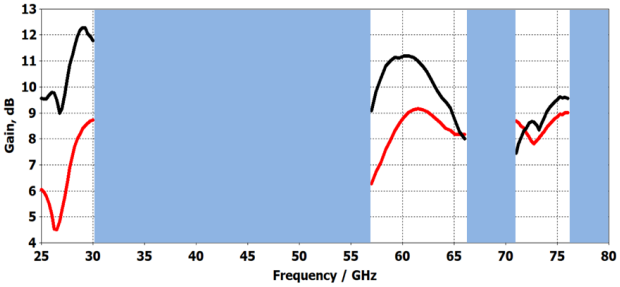

Figure. 13 Simulated Gain comparison of suggested combination, Red (without reflector) and Black (with reflector)

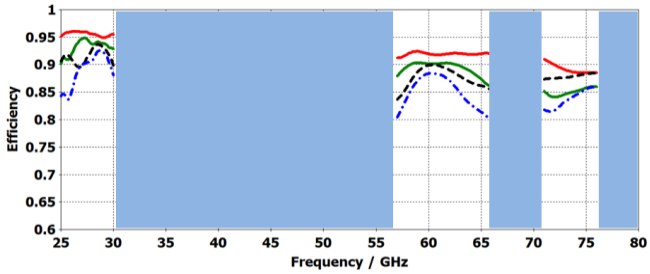

Figure. 14 Simulated efficiency comparison of suggested combination, red (Rad. Eff. without reflector), green (Rad. Eff. with reflector), black (Tot. Eff. without reflector), and blue (Tot. Eff. with reflector).

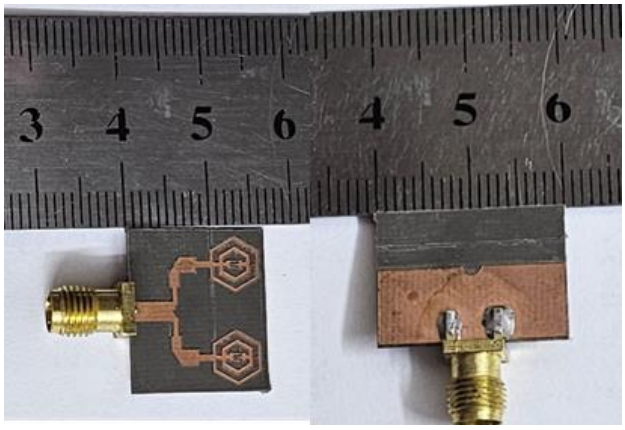

(a)

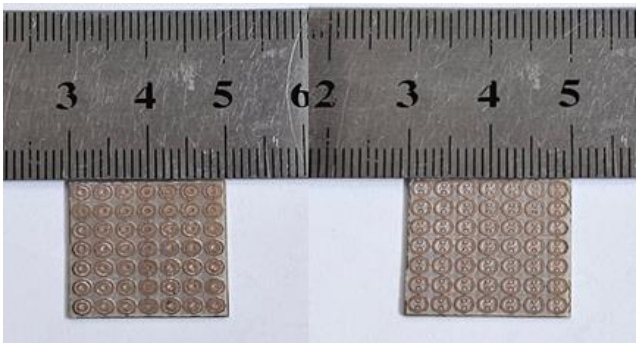

(b)

Figure. 15 Photo of the prototype: (a) Two element antenna design and (b) FSS-based reflector top and bottom view

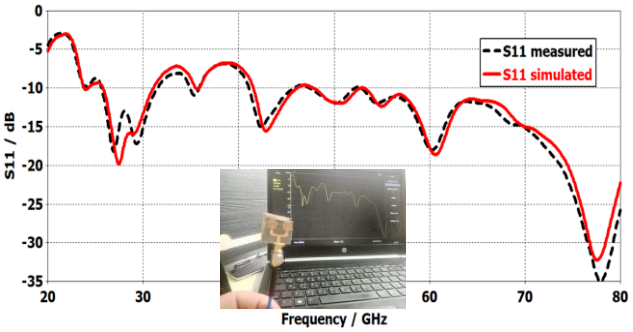

Figure. 16 S_{11} of the suggested antenna integrated with the proposed FSS reflector

5. Comparison with previous work

Table 3 provides a full comparison of the suggested antenna with and without the reflector to other relevant studies of antenna designs combined with different surfaces. The proposed antenna design with reflector offers several advantages. It has a significantly smaller size of 19.6 x 20 x 3.74 mm³ compared to the larger dimensions ranging from 27.8 x 10.2 x 3.5 mm³ to 66.75 x 28.75 x 6.679 mm³ for the other designs. The proposed design also achieves a wider bandwidth of 38.6 GHz, exceeding the others except [22] where it shows a bandwidth of 45 GHz. In terms of radiation efficiency, the proposed antenna reaches 90 % similar to the others. However, the proposed design does have a slightly lower peak gain of 11.1, 10.7 and 9.7 dBi compared to the higher gains of 15, 12, 11 dBi for [22] and 12.2 dBi for [33], likely due to the more compact size. Overall, the proposed antenna design represents a compelling trade-off, offering significant size and bandwidth advantages while maintaining high radiation efficiency, albeit at the expense of a modest reduction in maximum gain compared to some of the larger, higher-gain designs.

Table 2. Equivalent circuit components for FSS based reflector

Parameter	R1 (Ω)	L1 (nH)	C1 (fF)	R2 (Ω)	L2 (nH)	C2 (pF)
Value	512.6	132.56	33	152.5	6.2	0.0014
Parameter	R3 (Ω)	L3 (nH)	C3 (fF)	M1,2 (nH)	L_{SUBB} (nH)	C_{SUB} (pF)
Value	11.26	440.1	3	2.2	6.6	0.001

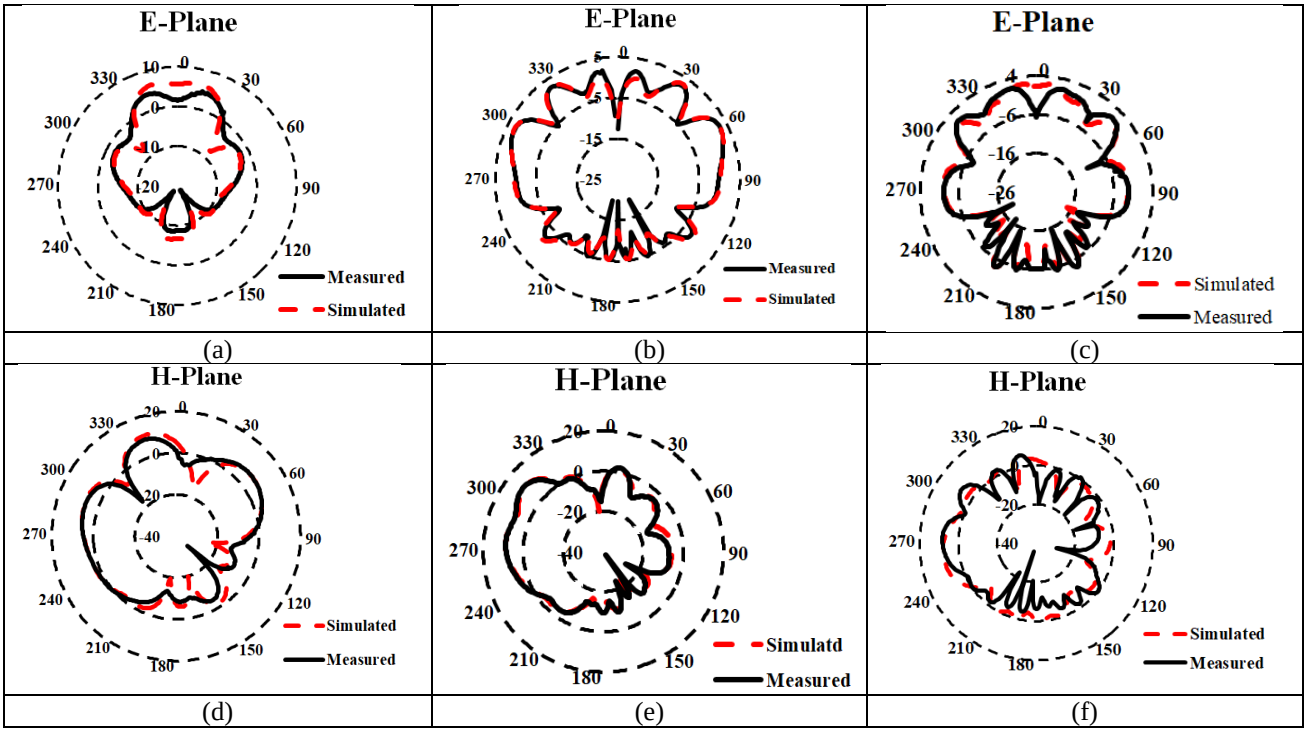

Figure. 17 The estimated and tested radiation patterns of proposed antenna with reflector at: (a) and (d) at 28 GHz, (b) and (e) at 60 GHz, and (c) and (f) at 73 GHz

Table 3. Comparison of suggested two-element antenna with other relevant designs

Ref.		**Antenna size (mm^3)**	**ε_r/thickness (mm)**	**Operating Band (GHz)**	**BW(GHz)**	**Array factor**	**Gain (dB)**	**Radiation Efficiency %**
This Work	w/o	16.5 x 20 x 0.87	2.2/0.8	28,60,73	6.2,32.4	2	6.7 ,8.7 ,8.5	92, 88, 90
	w	19.6 x20 x 3.74	4.3/0.8				11.1, 10.7, 9.5	90, 85, 86
[22]	w/o	66.75 × 28.75 x 0.875	2.2/0.787	28,38,60	45	8	12,10,9.5	N/A
	w	66.75 × 28.75 × 6.679	2.2/0.787				15,12,11	86,87,78
[30]	w/o	40 x 40 x 0.787	2.2/0.787	24.5	3	1	-	N/A
	w	40 x 40 x 14	2.2/0.787				12.2	N/A
[31]	w/o	27.8 x 10.2 x 0.508	3.38/0.508	28	6	1	10	N/A
	w	27.8 x 10.2 x 3.5	3.38/3.516				11	N/A
[32]	w/o	18 x 18 x 0.87	2.2/0.8	28	1.6	4	7.2	N/A
	w	45 x 45 x 8.94	2.2/0.8				8.6	N/A
[33]	w/o	12 x 12 x 0.203	3.55/0.203	28	3.8	1	4.5	93
	w	25 x 25 x 5	2.2/0.5				10.3	90

6. Conclusion

The objective of this work is to construct two-element antennas that meet the necessary gain targets for 5G applications. Even though the two-element antenna design increased gain levels at the desired frequencies, greater values were gained by integrating a FSS-based reflector. At 28 GHz, 60 GHz, and 73 GHz, respectively, the recommended two-element antenna with FSS-based reflector displayed adequate gain of 12 dBi, 11 dBi, and 9.5 dBi. Measurable outcomes were obtained once the proposed design was implemented. There was a strong agreement between the tested and simulation

outcomes. The suggested two-element array design's wide bandwidth, consistent radiation patterns, and suitable high gains at the desired bands make it an ideal antenna for 5G applications.

Conflicts of Interest

The authors declare no conflict of interest.

Acknowledgments

This work is supported by the College of Engineering/ Mustansiriyah University (https://webmain.uommustansiriyah.edu.iq).

Author Contributions

As the original author and corresponding author, Nada Nasih Tawfeeq studied and performed this work. Adheed Hassan Sallomi supervised, kept track the research and enhanced its scientific components.

References

[1] B. G. P. Shariff, T. Ali, P. R. Mane and P. Kumar, "Array Antennas for mmWave Applications: A Comprehensive Review", *IEEE Access*, Vol. 10, pp. 126728-126766, 2022,

[2] J. Zhang, X. Yu, and K. B. Letaief, "Hybrid beamforming for 5G and beyond millimeter-wave systems: A holistic view", *IEEE Open J. Commun. Soc.*, Vol. 1, No. November 2019, pp. 77–91, 2020.

[3] Q. Yang *et al.*, "Millimeter-Wave Dual-Polarized Differentially Fed 2-D Multibeam Patch Antenna Array", *IEEE Trans. Antennas Propag.*, vol. 68, no. 10, pp. 7007–7016, 2020.

[4] W. Hong *et al.*, "The Role of Millimeter-Wave Technologies in 5G/6G Wireless Communications", *IEEE J. Microwaves*, Vol. 1, No. 1, pp. 101–122, 2021.

[5] M. F. Khajeim, G. Moradi, R. S. Shirazi, S. Zhang, and G. F. Pedersen, "Wideband Vertically Polarized Antenna with Endfire Radiation for 5G Mobile Phone Applications", *IEEE Antennas Wirel. Propag. Lett.*, Vol. 19, No. 11, pp. 1948–1952, 2020.

[6] A. Abdelaziz, H. A. Mohamed, and E. K. I. Hamad, "Applying Characteristic Mode Analysis to Systematically Design of 5G Logarithmic Spiral MIMO Patch Antenna", *IEEE Access*, Vol. 9, pp. 156566–156580, 2021.

[7] H. Zahra, W. A. Awan, W. A. E. Ali, N. Hussain, S. M. Abbas, and S. Mukhopadhyay, "A 28 ghz broadband helical inspired end-fire antenna and its mimo configuration for 5g pattern diversity applications", *Electron.*, Vol. 10, No. 4, pp. 1–15, 2021.

[8] Z. Li *et al*., "A 39-GHz CMOS Bidirectional Doherty Phased- Array Beamformer Using Shared-LUT DPD With Inter-Element Mismatch Compensation Technique for 5G Base Station", *IEEE Journal of Solid-State Circuits*, Vol. 58, No. 4, pp. 901-914, April 2023.

[9] C. W. Byeon, "A 28 GHz Highly Linear Up-Conversion Mixer for 5G Cellular Communications", *Technologies*, Vol. 12, No. 3, 2024.

[10] R. K. Saha, "Coexistence of Cellular and IEEE 802.11 Technologies in Unlicensed Spectrum Bands -A Survey", *IEEE Open J. Commun. Soc.*, Vol. 2, No. August, pp. 1996–2028, 2021.

[11] J. Wells, "New Multi-Gigabit Wireless Systems Satisfy High-Security Rapid Response Applications", *Mil. Embed. Syst.*, pp. 1–4, 2006.

[12] A Kumar , A. Kumar, and A. Kumar, "Gain enhancement of a wideband rectangular ring monopole millimeter-wave antenna using artificial magnetic conductor structure", *Int J RF Microw Comput Aided Eng.*, Vol. 23, 2022.

[13] A. A. Althuwayb, "MTM-and SIW-Inspired Bowtie Antenna Loaded with AMC for 5G mm-Wave Applications", *Int. J. Antennas Propag.*, Vol. 2021, 2021.

[14] D. Bean and J. Venkataraman, "Gain Enhancement of On-Chip Antenna at 60 GHz Using an Artificial Magnetic Conductor", In: *Proc. of IEEE International Symposium on Antennas and Propagation and North American Radio Science Meeting*, pp. 1423-1424, 2020.

[15] W. A. E. Ali, A. A. Ibrahim, and A. E. Ahmed, *Dual-Band Millimeter Wave 2 × 2 MIMO Slot Antenna with Low Mutual Coupling for 5G Networks*, *Springer* US, 2023.

[16] I. Meates, S. Alkaraki, M. Aslam, Q. Abbasi, A. Evans and S. F. Jilani", A Compact High-Gain 28 GHz Antenna Array for Beyond 5G Wireless Networks", In: *Proc. of 2024 18th European Conference on Antennas and Propagation (EuCAP)*, Glasgow, UK, pp. 1-3, 2024.

[17] A. Jabbar, Q. Abbasi, Z. Pang, M. A. Imran and M. Ur-Rehman, "High Performance 60 GHz Beamforming Antenna Array For 5G and Beyond Industrial Applications", In: *Proc. of 17th European Conference on Antennas and Propagation (EuCAP)*, Glasgow, UK, pp. 1-5, 2023.

[18] A. Kumar and G. P. Pandey, "A Narrow Beam Gain Enhanced Wideband Antenna Array Using Slits, I-Slots, and L-Shaped Reflector for 5G

Millimeter Wave Applications", *International Journal of RF and Microwave Computer-Aided Engineering*, 11 pages, 2024.

[19] S. Tariq, W. T. Sethi and A. A. Rahim, "High Gain Dual-band Compact Antenna Array for Millimeter Wave Applications", In: *Proc. of 10th International Conference on Wireless Networks and Mobile Communications (WINCOM)*, Istanbul, Turkiye, pp 1-6, 2023.

[20] T. Hossain et al, "Performance Enhancement of UWB Antenna Using FSS Layer for millimeter-wave 5G", In: *Proc. of International Conference on Next-Generation Computing, IoT and Machine Learning (NCIM)*, Gazipur, Bangladesh, pp. 1-6, 2023.

[21] P. P. Mohammadi, H. Naseri, N. Melouki, F. Ahmed, M S. Bizan, A. Iqbal and T. A. Denidni, "A Fabry–Perot antenna using a frequency selective surface layer with wideband and Low RCS for Mm-wave applications", *AEU - International Journal of Electronics and Communications*, Vol.169, 2023.

[22] R. Ullah *et al.*, "Wideband and high gain array antenna for 5G smart phone applications using frequency selective surface", *IEEE Access*, Vol. 10, No. July, pp. 86117–86126, 2022.

[23] N. N. Tawfeeq and A. H. Sallomi, "Tri-Band Two Rings Antenna Loaded with Inter Digital Capacitor for Fifth Generation Applications", *Journal of Engineering and Sustainable Development (JEASD)*, Vol. vx, No. xx, pp. 1–9.

[24] J. Wiley, *Antenna Theory Analysis and Design Third Edition (BOOK)*, 2005.

[25] B. De M. Pinheiro *et al.*, "The influence of antenna gain and beamwidth used in OSSEUS in the screening process for osteoporosis", *Sci. Rep.*, Vol. 11, No. 1, pp. 1–19, 2021.

[26] S.S. Gültekin, and M. Yerlikaya, "Enhanced Gain Dual-Port Compact Printed Meandered Log-Periodic Monopole Array Antenna Design with Octagonal-Ring Shaped FSS for Broadband 28 GHz Applications", *Arab J Sci Eng.*, 2024.

[27] S. Ghosh and K. V. Srivastava, "An equivalent circuit model of FSS-based metamaterial absorber using coupled line theory", *IEEE Antennas Wirel. Propag. Lett.*, Vol. 14, No. c, pp. 511–514, 2015.

[28] M. M. Hasan *et al.*, "Polarization insensitive dual band metamaterial with absorptance for 5G sub-6 GHz applications", *Sci. Rep.*, Vol. 12, No. 1, pp. 1–20, 2022.

[29] R. S. Anwar, Y. Wei, L. Mao, and H. Ning, "Miniaturised frequency selective surface based on fractal arrays with square slots for enhanced bandwidth", *IET Microwaves, Antennas Propag.*, Vol. 13, No. 11, pp. 1811–1819, 2019.

[30] F. Guidoum, M. L. Tounsi, T. Vuong, N. Ababou, and M. C. Yagoub, "Enhancing 5G antenna performance by using 3D FSS structures", *International Journal of RF and Microwave Computer-Aided Engineering*, Vol. 31, No. 8, 2021.

[31] M. Mantash, A. Kesavan, and T. A. Denidni, "Beam-Tilting Endfire Antenna Using a Single-Layer FSS for 5G Communication Networks", *IEEE Antennas Wirel. Propag. Lett.*, Vol. 17, No. 1, pp. 29–33, 2018.

[32] I. Ud Din *et al.*, "Frequency-Selective Surface-Based MIMO Antenna Array for 5G Millimeter-Wave Applications", *Sensors*, Vol. 23, No. 15, pp. 1–17, 2023.

[33] H. A. Mohamed, M. Edries, M. A. Abdelghany, and A. A. Ibrahim, "Millimeter-Wave Antenna With Gain Improvement Utilizing Reflection FSS for 5G Networks", *IEEE Access*, Vol. 10, No. July, pp. 73601–73609, 2022.